An introduction to OFDM – modeling and implementation

$f_n = f_0 + n f_\Delta, \;\; n = 0,1, \dots, K-1$

$f_n = f_{rc} + g_n f_\Delta, \;\; n = 0,1, \dots, K-1$

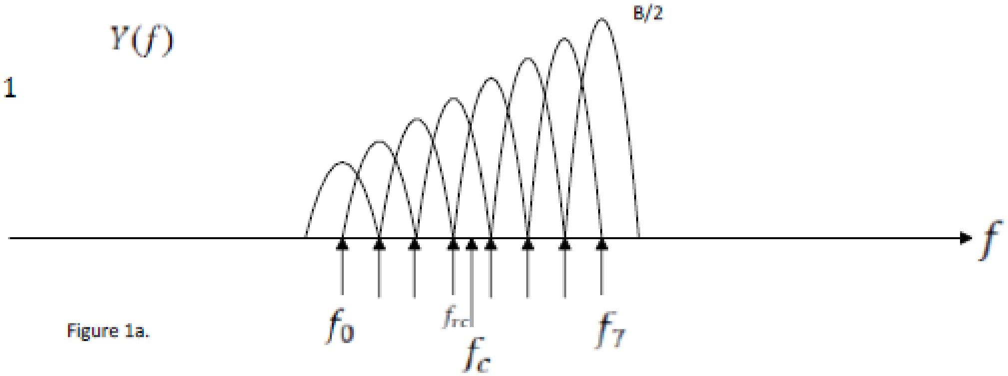

Figure 1a.

$g_0 f_\Delta, \dots, -f_\Delta, 0, f_\Delta, \dots \dots, g_{K-1} f_\Delta$

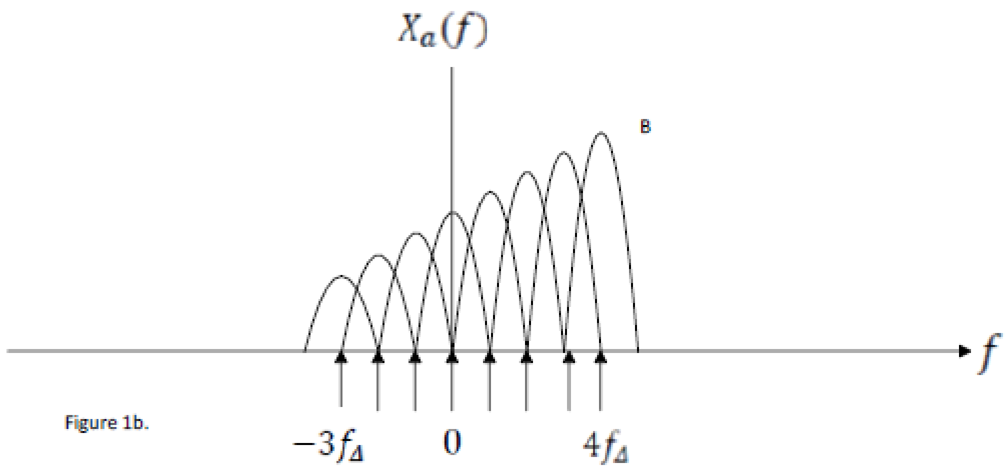

Figure 1b.

$$y(t) = Re\{\sum_{n=0}^{K-1} a_n e^{j2\pi g_n f_\Delta t} e^{j2\pi f_{rc} t}\} = Re\{x(t) e^{j2\pi f_{rc} t}\}$$

$$x(t) = x_{Re}(t) + j x_{Im}(t) = \sum_{n=0}^{K-1} a_n e^{j2\pi g_n f_\Delta t}, \qquad 0 \le t \le T_{obs} \qquad (2.3)$$

Note that $y(t)$ in equation (2.2) can be written as,

$$y(t) = Re\{x(t) e^{j2\pi f_{rc} t}\} = x_{Re}(t)\cos(2\pi f_{rc} t) - x_{Im}(t)\sin(2\pi f_{rc} t) \qquad (2.5)$$

$$f_{samp} = N/T_{obs} = N f_\Delta > K f_\Delta$$

$$x_m = x(mT_{obs}/N) = \sum_{n=0}^{K-1} a_n e^{j2\pi g_n m/N} \qquad m = 0,1 \dots, (N-1)$$

$$X(v) = \sum_{n=0}^{N-1} x_n e^{-j2\pi v n}$$

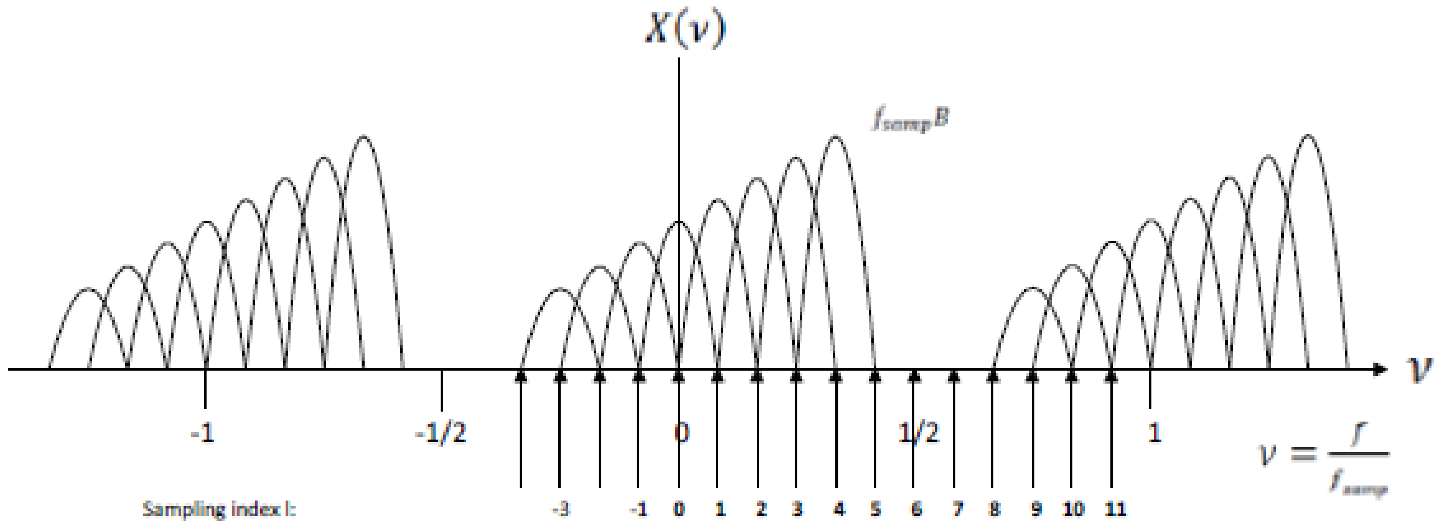

$$X_k = X(\nu = k/N) = \sum_{n=0}^{N-1} x_n e^{-j2\pi kn/N}, k = 0,1,\dots,N-1 \qquad \textbf{(DFT)}$$

$$x_n = \frac{1}{N}\sum_{k=0}^{N-1} X_k e^{j2\pi kn/N}, n = 0,1,\dots,N-1 \qquad \textbf{(IDFT)}$$

Consider as an example the case K=8 and N=12. In this case $n_{rc} = 3$ and $g_{K-1} = 4$, and the desired sequence $X_0, X_1, \dots, X_{11}$ then equals: $Na_3, Na_4, Na_5, Na_6, Na_7, 0,0,0,0, Na_0, Na_1, Na_2$. See also figure 4.

$$X_l = Na_{n_{rc}+l} \qquad l = 0,1 \dots , g_{K-1} \tag{2.23}$$

$$X_{-n_{rc}+N+n} = Na_n \qquad n = 0,1, \dots (n_{rc} - 1) \tag{2.25}$$

If we first construct the size-N sequence $Na_0, Na_1, \dots, Na_{K-1}, 0,0, \dots, 0$, and then "left-rotate" this sequence n_{rc} positions (or "right-rotate" this sequence $(g_0 + N)$ positions), then the desired sequence $X_0, X_1, \dots, X_{N-1}$ in equations (2.20)-(2.25) is obtained!

The final step is to calculate the size-N **IDFT**,

$$x_n = \frac{1}{N} \sum_{k=0}^{N-1} X_k e^{j2\pi kn/N} , n = 0,1, \dots , N - 1 \tag{2.26}$$

In practice, **N is a power of 2** since fast Fourier transform (FFT) algorithms can then be used to significantly speed up the calculations in equation (2.26).

3. The Cyclic Prefix (CP) and Digital-to-Analog (D/A) conversion

Now observe that the signal $x(t)$ in equation (2.3) has duration T_{obs}. However, the expression that is used to define $x(t)$ equals $\sum_{n=0}^{K-1} a_n e^{j2\pi g_n f_\Delta t}$, and this expression is **periodic in t with period T_{obs}**.

Based on the discussion about periodicity above let us therefore construct a new size-(L+N) vector $\boldsymbol{u}$ as a so-called *periodic extension* of the size-N vector **x**. This means that *the L last samples in $\boldsymbol{x}$ are copied and placed as the first L samples in $\boldsymbol{u}$*. The remaining N samples in $\boldsymbol{u}$ are identical to $\boldsymbol{x}$. This

$$u(t) = u_{Re}(t) + j u_{Im}(t) = \sum_{n=0}^{K-1} a_n e^{j2\pi g_n f_\Delta (t - T_{CP})}, \quad 0 \leq t \leq T_s$$

$$s(t) = Re\{u(t) e^{j2\pi f_{rc} t}\} = u_{Re}(t)\cos(2\pi f_{rc} t) - u_{Im}(t)\sin(2\pi f_{rc} t)$$

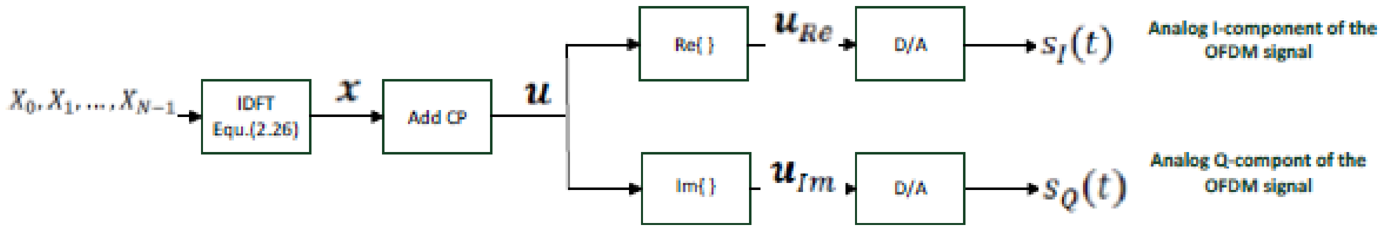

Figure 5. Block diagram illustrating the operations in the digital domain, and the transition to the analog domain.

$$s_I(t) = \sum_{m=0}^{L+N-1} u_{Re,m}\, g_i(t - \frac{mT_{obs}}{N})$$

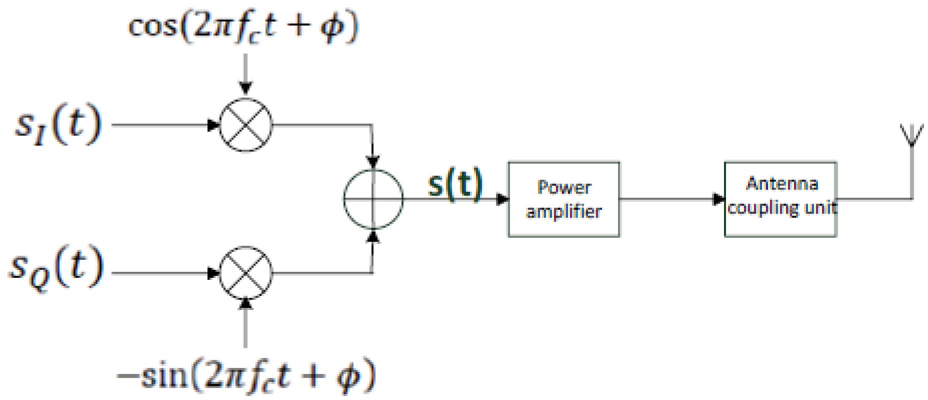

Figure 6. Block diagram illustrating frequency up-converting to the carrier frequency (K is odd), the power amplifier, and the antenna coupling unit. The OFDM signal $s(t)$ is given in equation (4.1).

5. The multi-path (linear time-invariant filter) channel, and the additive white Gaussian noise (AWGN)

INPUT OFDM: $As(t) = ARe\{\sum_{n=0}^{K-1} a_n \, e^{j(2\pi f_n t+\theta_n)}\},$

OUTPUT OFDM: $z(t) = ARe\{\sum_{n=0}^{K-1} a_n H(f_n) \, e^{j(2\pi f_n t+\theta_n)}\},$ $\quad T_{CP} \leq t \leq T_s$ (5.13)

6. The Receiver: Frequency down-converting, sampling (A/D) and the DFT

$$r(t) = b_I \cos(2\pi f_B t) - b_Q \sin(2\pi f_B t) + n(t)\,,\ \ 0 \le t \le T$$

$$\psi_1(t) = \cos(2\pi f_B t)/C\,, \qquad 0 \le t \le T$$

$$\psi_2(t) = -\sin(2\pi f_B t)/C\,, \qquad 0 \le t \le T$$

$$r_1 = \int_0^T r(t)\psi_1(t)\,dt = Cb_I + n_1 \qquad r_2 = \int_0^T r(t)\psi_2(t)\,dt = Cb_Q + n_2$$

$$r = r_1 + jr_2 = \int_0^T r(t)e^{-j2\pi f_B t}\,dt/C = R(f_B)/C = Cb + n$$

It is now very important to observe in equation (6.8) that **the received noisy signal point r can be found by calculating the Fourier transform $R(f)$ of the received signal $r(t)$ over the time interval $0 \le t \le T$, and then sample $R(f)$ at $f = f_B$ to obtain $R(f_B)$.** As will be seen later on, *using the DFT in an OFDM receiver can be viewed as a natural extension of this result.* This concludes the example, and it is time to focus on frequency down-converting to baseband.

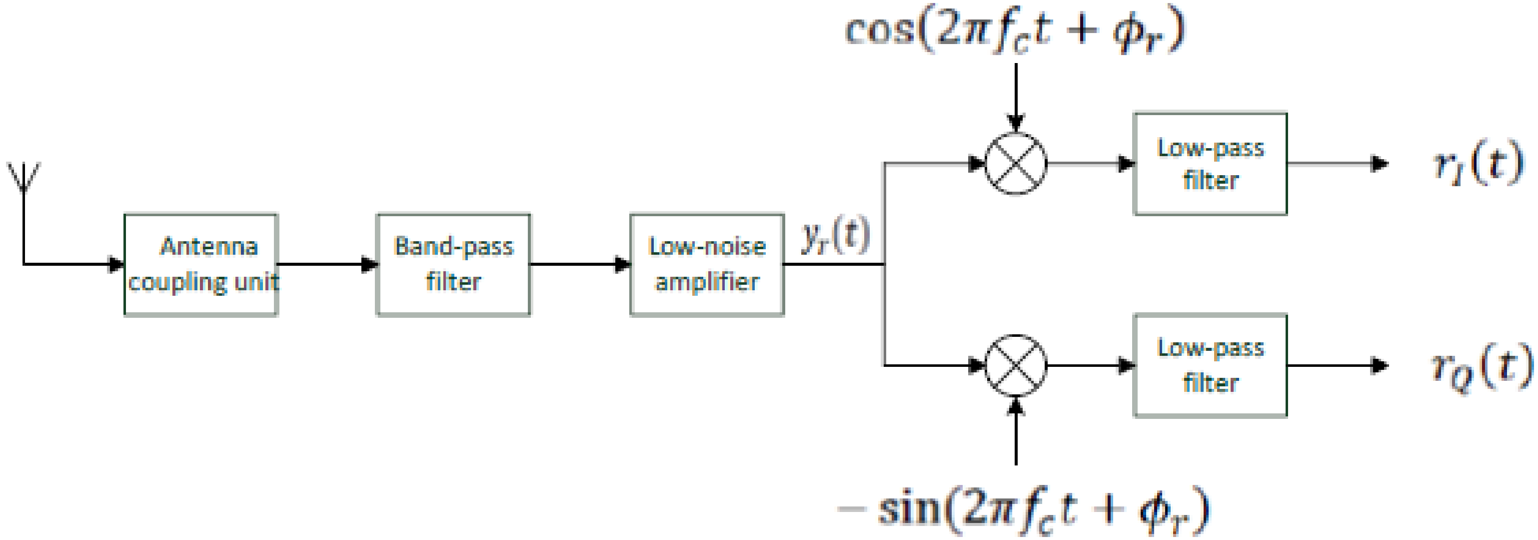

Figure 8. Illustrating the first part of the receiver: the antenna coupling unit, band-pass filter (wide), low-noise amplifier (LNA) and a homodyne unit for frequency down-converting and extracting the baseband signals $r_I(t)$ and $r_Q(t)$. It is here assumed that K is odd for which $f_{rc} = f_c$.

$$r_I(t) + jr_Q(t) = \sum_{n=0}^{K-1} a_n H_{eq}(f_n) e^{j2\pi g_n f_\Delta (t-T_{CP})} + w(t), \quad T_{CP} \le t \le T_s \tag{6.15}$$

$$H_{eq}(f_n) = H_{eq,n} = AH(f_n)e^{j\phi}G_1(f_n)e^{-j\phi_r}G_{lp}(f_n - f_{rc} = g_n f_\Delta)/2 \tag{6.16}$$

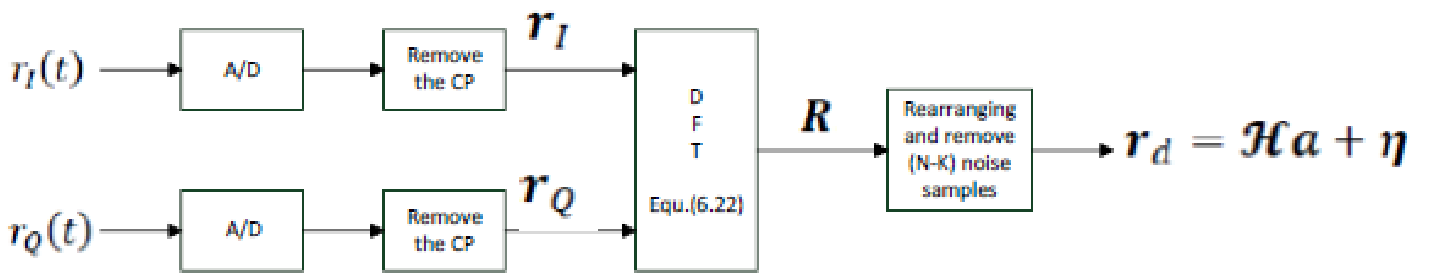

$$r_{I,m} = r_I((L+m)T_{obs}/N), \quad m = 0,1,\dots,N-1$$

$$r_{Q,m} = r_Q((L+m)T_{obs}/N), \quad m = 0,1,\dots,N-1$$

$$\boldsymbol{r} = \boldsymbol{r}_I + j\boldsymbol{r}_Q$$

From equation (6.15) it is seen that the discrete-time signal $\boldsymbol{r}$ is a sampled version of the complex signal $x_r(t)$, where $x_r(t)$ is defined as,

$$x_r(t) = r_I(t+T_{CP}) + jr_Q(t+T_{CP}) = \sum_{n=0}^{K-1} a_n H_{eq,n} e^{j2\pi g_n f_\Delta t} + w'(t), \quad 0 \le t \le T_{obs} \quad (6.20)$$

The signal $x_r(t)$ in equation (6.20) should be compared with the signal $x(t)$ in equation (2.3) on page 6!

Let us therefore calculate the size-N DFT of the discrete-time signal $\boldsymbol{r}$,

$$R_k = R(\nu = k/N) = \sum_{n=0}^{N-1} r_n e^{-j2\pi kn/N}, k = 0,1,\dots,N-1 \quad (6.22)$$

We can now write $\boldsymbol{R}$ as,

$$\boldsymbol{R} = \boldsymbol{X}_r + \boldsymbol{w}_r \tag{6.24}$$

where $\boldsymbol{X}_r$ is the noise-free part of $\boldsymbol{R}$, and $\boldsymbol{w}_r$ is the noise vector.

As an example, the first value $X_{r,0}$, which is contained in the frequency sample $R_0 = R(\nu = 0)$, equals $X_{r,0} = a_{n_{rc}} H_{eq,n_{rc}}$.

$$(\boldsymbol{\mathcal{H}} \boldsymbol{a})^{tr} = (a_0 H_{eq,0} \;\; a_1 H_{eq,1} \; \dots . \, a_{K-1} H_{eq,K-1})$$

$$\boldsymbol{X}_r = N \boldsymbol{Q}_t \boldsymbol{\mathcal{H}} \boldsymbol{a} \tag{6.26}$$

To recover the K received noisy signal points we "re-rotate" the vector $\boldsymbol{R}$ according to equation (2.30),

$$\boldsymbol{r}_d = \frac{1}{N} \boldsymbol{Q}_r \boldsymbol{R} = \boldsymbol{Q}_r \boldsymbol{Q}_t \boldsymbol{\mathcal{H}} \boldsymbol{a} + \frac{1}{N} \boldsymbol{Q}_r \boldsymbol{w}_r = \boldsymbol{\mathcal{H}} \boldsymbol{a} + \boldsymbol{\eta} \tag{6.28}$$

Observe that the elements in the size-K column vector $\boldsymbol{r}_d$ *are the desired received distorted and noisy signal points*,

$$r_{d,n} = a_n H_{eq,n} + \eta_n, \quad n = 0,1, \dots, (K-1) \tag{6.29}$$

7. An alternative transmitter implementation using a higher sampling frequency

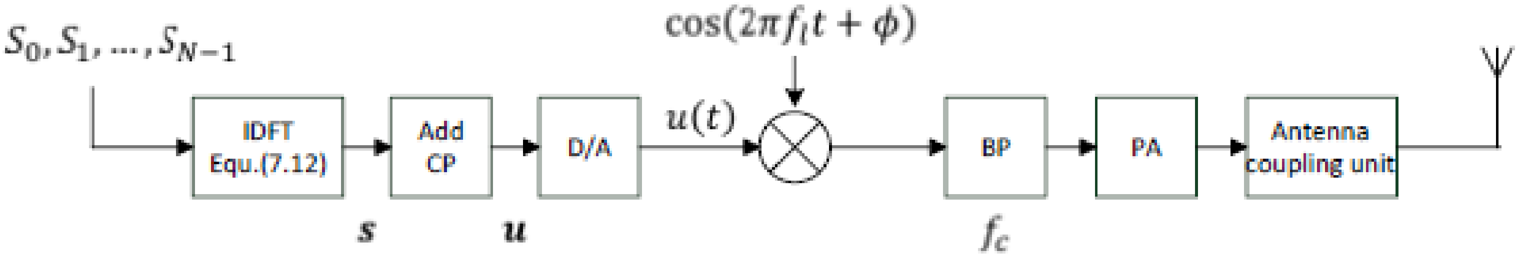

Figure 10. Illustrating how to create the OFDM signal $u(t)$ in equation (7.15). The size-N IDFT is used and N is given by equation (7.4). The construction of the sequence $S_0, S_1, \ldots, S_{N-1}$ is given by equations (7.10)-(7.11). This figure also includes a possible frequency up-converting to a higher carrier frequency f_c. The band-pass (BP) filter is centered around f_c, and PA means the power amplifier.

$$s(t) = g_{rec}(t) Re\{\sum_{n=0}^{K-1} a_n e^{j2\pi(f_0+nf_\Delta)t}\} \quad (7.1)$$

The frequency content, for positive frequencies, is roughly indicated in Figure 1.1a on page 7. A significant difference however, compared to section 1 is that here we assume that the K sub-carriers in the OFDM signal $s(t)$ have relatively **low frequencies**. More specifically it is here assumed that the sub-carrier f_0 equals,

$$f_0 = N_g f_\Delta \quad (7.2)$$

The OFDM signal $s(t)$ in equation (7.1) can be expressed in the following way within the time-interval $0 \leq t \leq T_{obs}$,

$$s(t) = g_{rec}(t) Re\{\sum_{n=0}^{K-1} a_n e^{j2\pi(f_0+nf_\Delta)t}\} = \frac{g_{rec}(t)}{2} (\sum_{n=0}^{K-1} a_n e^{j2\pi(f_0+nf_\Delta)t} + \sum_{n=0}^{K-1} a_n^* e^{-j2\pi(f_0+nf_\Delta)t}) \quad (7.3)$$

$f_{samp} = Nf_\Delta$ where,

$$N > 2(N_g + K) \quad (7.4)$$

Let the vector $\boldsymbol{s}$ contain the N *real* samples $s_0, s_1, \dots, s_{N-1}$, of the signal $s(t)$, where

$$s_m = s(mT_{obs}/N) = \frac{1}{2}\left(\sum_{n=0}^{K-1} a_n e^{j2\pi(f_0+nf_\Delta)mT_{obs}/N} + \sum_{n=0}^{K-1} a_n^* e^{-j2\pi(f_0+nf_\Delta)mT_{obs}/N}\right) \qquad (7.5)$$

This can be simplified to,

$$s_m = s(mT_{obs}/N) = \frac{1}{2}\left(\sum_{n=0}^{K-1} a_n e^{\frac{j2\pi(N_g+n)m}{N}} + \sum_{n=0}^{K-1} a_n^* e^{-\frac{j2\pi(N_g+n)m}{N}}\right), m = 0,1,\dots,(N-1) \qquad (7.6)$$

$$S(\nu) = \sum_{n=0}^{N-1} s_n e^{-j2\pi\nu n} \qquad (7.7)$$

$$S_k = S(\nu = k/N) = \sum_{n=0}^{N-1} s_n e^{-j2\pi kn/N}, k = 0,1,\dots,N-1 \qquad \textbf{(DFT)} \qquad (7.8)$$

$$S_{N_g+k} = Na_k, \ \ 0 \le k \le K-1 \tag{7.10}$$

$$S_{N_g+K+N_x+k} = Na^*_{K-1-k}, \quad 0 \le k \le K-1 \tag{7.11}$$

For the remaining $(N-2K)$ samples in the sequence $S_0, S_1, \dots, S_{N-1}$ the value equals zero.

Consider as an example the case K=3, $N_g = 2$ and N=12. In this case the desired sequence $S_0, S_1, \dots, S_{11}$ then equals: $0,0, Na_0, Na_1, Na_2, 0,0,0, Na_2^*, Na_1^*, Na_0^*, 0$.

Hence, the sequence of samples $S_0, S_1, \dots, S_{N-1}$ is completely determined and the desired real sequence $\boldsymbol{s}$ is found from the size-N IDFT,

$$s_n = \frac{1}{N}\sum_{k=0}^{N-1} S_k e^{j2\pi kn/N}, n = 0,1,\dots,N-1 \qquad \textbf{(IDFT)} \qquad (7.12)$$

8. An alternative receiver implementation using a higher sampling frequency

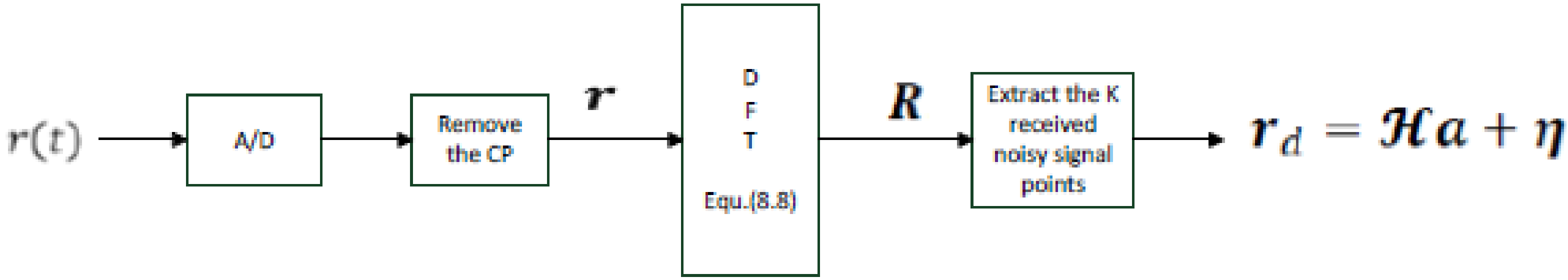

Figure 11. Illustrating a possible way to extract the K received noisy signal points if a high sampling frequency is used. The real noisy OFDM signal $r(t)$ is given in equation (8.1), and it is assumed to be available at a certain stage in the receiver. The size-N DFT is used and N is given by equation (8.4). The final result $\boldsymbol{r}_d$ is given in equations (8.11)-(8.13).

Chapter 9

An Introduction to Time-varying Multipath Channels

$$\boxed{z(t) = \sum_n \alpha_n(t) s(t - \tau_n(t))} \qquad (9.1)$$

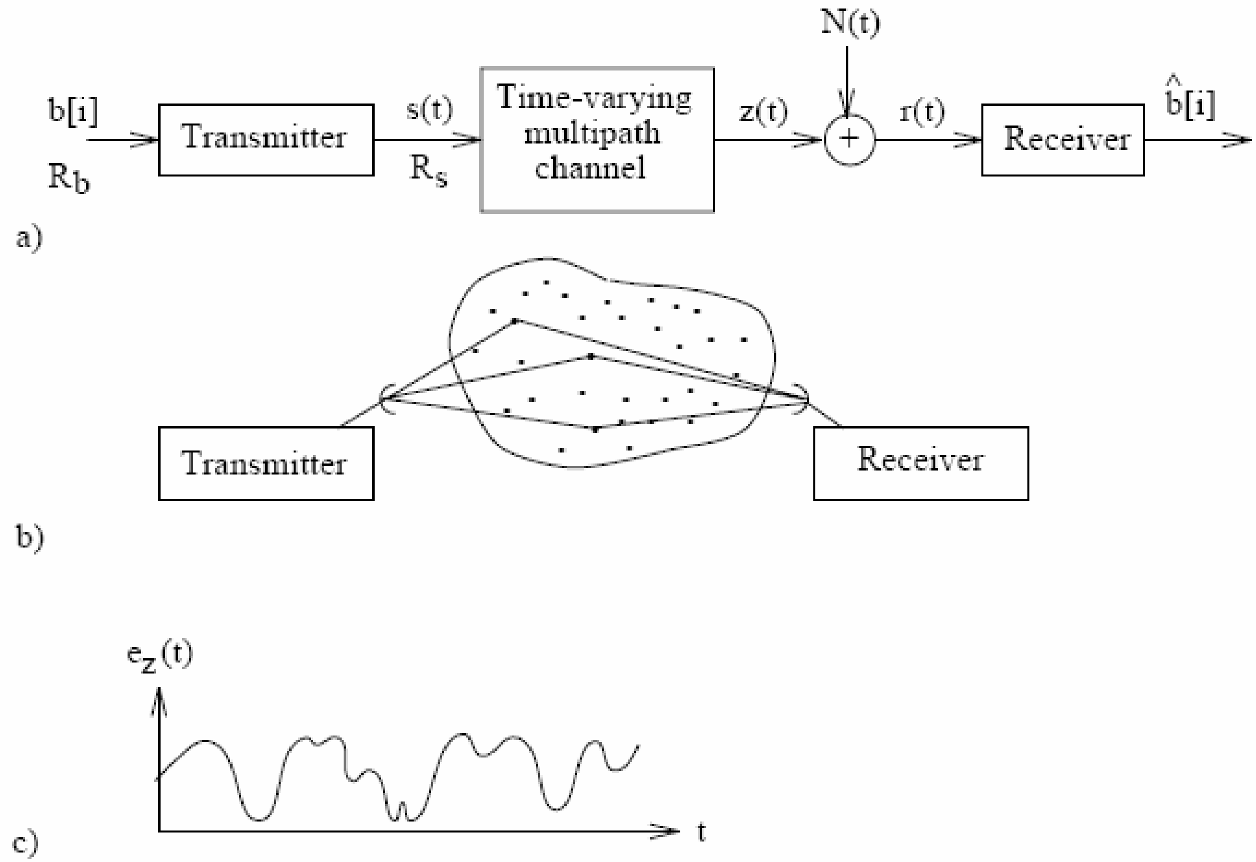

Figure 9.1: a) The digital communication system; b) A scattering medium; c) Illustrating the fading envelope $e_z(t)$.

$$s(t) = \cos((\omega_c + \omega_1)t) \; , \quad -\infty \le t \le \infty \tag{9.2}$$

$$\begin{aligned}
z(t) &= \sum_n \alpha_n(t) \cos((\omega_c + \omega_1)(t - \tau_n(t))) = \\
&= \underbrace{\left[\sum_n \alpha_n(t) \cos((\omega_c + \omega_1)\tau_n(t)) \right]}_{z_I(t) = \tilde{H}_{Re}(f_1, t)/2} \cos((\omega_c + \omega_1)t) - \\
&\quad - \underbrace{\left[\sum_n \alpha_n(t) \sin(-(\omega_c + \omega_1)\tau_n(t)) \right]}_{z_Q(t) = \tilde{H}_{Im}(f_1, t)/2} \sin((\omega_c + \omega_1)t) \\
&= z_I(t) \cos((\omega_c + \omega_1)t) - z_Q(t) \sin((\omega_c + \omega_1)t) \\
&= e_z(t) \cos((\omega_c + \omega_1)t + \theta_z(t)) \qquad (9.3)
\end{aligned}$$

Compare with the time-invariant QAM-result:

$$\begin{aligned}
A_z + jB_z &= (A + jB)H(f_c) = \sqrt{A^2 + B^2}|H(f_c)|e^{j(\nu + \phi(f_c))} = \\
&= (A + jB)(H_{Re}(f_c) + jH_{Im}(f_c)) \qquad (3.110)
\end{aligned}$$

$$s(t) = \cos((\omega_c + \omega_1)t) \ , \quad -\infty \leq t \leq \infty \tag{9.2}$$

$$\begin{aligned} z(t) &= \sum_n \alpha_n(t) \cos((\omega_c + \omega_1)(t - \tau_n(t))) = \\ &= e_z(t) \cos((\omega_c + \omega_1)t + \theta_z(t)) \end{aligned} \tag{9.3}$$

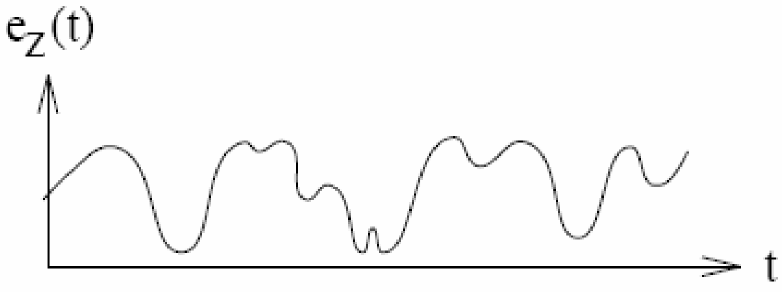

Observe that the quadrature components $z_I(t)$ and $z_Q(t)$ in (9.3) are *time-varying*. Hence, the output signal $z(t)$ is *not* a pure sine wave with frequency $f_c + f_1$. ***This is a significant difference compared with the linear time-invariant channel.*** It is seen in (9.3) that the quadrature components depend

$$
\begin{aligned}
z(t) &= \sum_n \alpha_n(t)\cos((\omega_c+\omega_1)(t-\tau_n(t))) = \\
&= z_I(t)\cos((\omega_c+\omega_1)t) - z_Q(t)\sin((\omega_c+\omega_1)t) \\
&= e_z(t)\cos((\omega_c+\omega_1)t+\theta_z(t))
\end{aligned}
$$

Throughout this chapter it is assumed that $z_I(t)$ and $z_Q(t)$ may be modelled as baseband zero-mean wide-sense-stationary (WSS) *Gaussian random processes* (with variances $\sigma_I^2 = \sigma_Q^2 = \sigma^2$). This is a commonly used assumption when the number of scatterers is large, implying that central limit theorem arguments can be used [43], [65], [68], [39]. For a fixed value of t, this assumption leads to a Rayleigh-distributed envelope $e_z(t)$,

$$e_z(t) = \sqrt{z_I^2(t) + z_Q^2(t)} \tag{9.4}$$

$$p_{e_z}(x) = \frac{2x}{b}\, e^{-x^2/b}, \quad x \geq 0\ , \text{ Rayleigh distr.} \tag{9.5}$$

$$b = E\{e_z^2(t)\} = 2\sigma^2 = 2P_z \tag{9.6}$$

and a uniformly distributed phase $\theta_z(t)$ (over a 2π interval). The zero-mean assumption means that there is no deterministic signal path present in $z(t)$. If a

9.1.1 Doppler Power Spectrum and Coherence Time

$$\boxed{\begin{aligned} R_{\mathcal{D}}(f) &= \mathcal{F}(\tilde{c}_z(\tau)) \\ \tilde{c}_z(\tau) &= \frac{1}{2}\, E\{[z_I(t+\tau) + jz_Q(t+\tau)]\ [z_I(t) - jz_Q(t)]\} \\ R_z(f) &= \frac{1}{2}\ (R_{\mathcal{D}}(f+f_c+f_1) + R_{\mathcal{D}}(f-f_c-f_1)) \end{aligned}} \qquad (9.7)$$

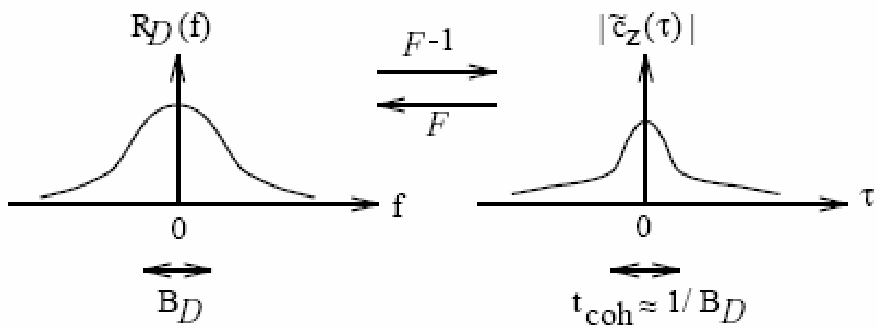

Figure 9.2: Illustrating the Fourier transform pair $\tilde{c}_z(\tau) \longleftrightarrow R_{\mathcal{D}}(f)$.

$$t_{coh} \approx 1/B_{\mathcal{D}} \qquad (9.8)$$

If the channel is slowly changing, then the coherence time is large. Note that $z_I(t+\tau)$ and $z_I(t)$ (also $z_Q(t+\tau)$ and $z_Q(t)$) are correlated over time-intervals τ (much) smaller than the coherence time t_{coh}. Hence, input signals within such intervals are therefore affected similarly by the fading channel. On the other hand, input signals that are separated in time by (much) more than t_{coh}, are affected differently by the channel, and at the output of the channel they become essentially independent of each other. If the former case apply (time flat fading), for a given time-interval, then we say that the channel is **time-nonselective**, and if the latter case apply, then the channel is said to be **time-selective**.

9.1.2 Coherence Bandwidth and Multipath Spread

$$z(t) = z(f_1, t) = \underbrace{\frac{1}{2}\,\tilde{H}_{Re}(f_1, t)}_{z_I(t)} \cos((\omega_c + \omega_1)t) - \underbrace{\frac{1}{2}\,\tilde{H}_{Im}(f_1, t)}_{z_Q(t)} \sin((\omega_c + \omega_1)t) \tag{9.9}$$

What can be said about the output signal $z(t)$ if another frequency $f_2 = f_1 + f_\Delta$ is used, instead of f_1? Are different frequency-intervals, in the input signal spectrum, treated differently by the time-varying multipath channel? To answer these questions the correlation between $z(f_1, t)$ and $z(f_1 + f_\Delta, t)$ can be found by

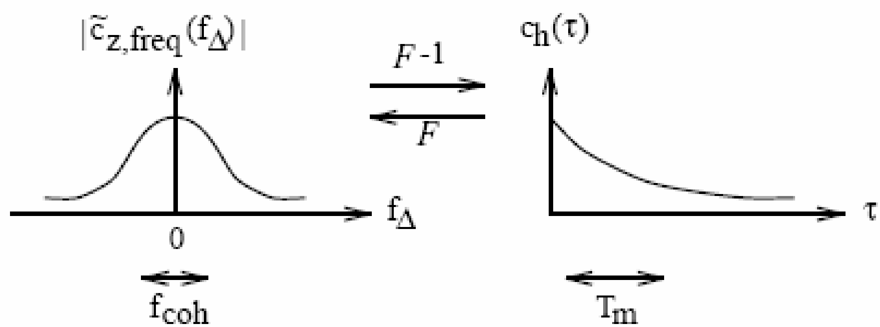

Figure 9.3: Illustrating the Fourier transform pair $c_h(\tau) \longleftrightarrow \tilde{c}_{z,freq}(f_\Delta)$.

The **coherence bandwidth f_{coh}** of the channel is defined as the width of the autocorrelation function $\tilde{c}_{z,freq}(f_\Delta)$, see Figure 9.3. Note that frequencies within a frequency-interval (much) smaller than the coherence bandwidth f_{coh} are correlated, and they are affected similarly by the fading channel. On the other hand, two frequencies that are separated by (much) more than f_{coh}, are affected differently by the channel, and they are essentially independent of each other. If the former case apply (frequency flat fading), for a given frequency-interval, then we say that the channel is **frequency-nonselective**, and if the latter case apply, then the channel is said to be **frequency-selective**.

$$\boxed{z(t) = \int_{-\infty}^{\infty} h(\tau, t) s(t - \tau) d\tau} \quad (9.10)$$

delay power spectrum $c_h(\tau)$ (also multipath intensity profile) of the time-varying impulse response $h(\tau, t)$,

$$c_h(\tau) = E\left\{\frac{h^2(\tau, t)}{2}\right\} = \frac{1}{2}\, E\{h_I^2(\tau, t) + h_Q^2(\tau, t)\} = \frac{1}{2}\, E\{\tilde{h}(\tau, t)\tilde{h}^*(\tau, t)\} \quad (9.15)$$

An example of the delay power spectrum $c_h(\tau)$ is illustrated in Figure 9.3. The width of the delay power spectrum is referred to as the **multipath spread** of the channel and it is denoted by T_m. This is an important parameter since if T_m is too large, compared with e.g. the symbol time, then intersymbol interference can occur.

$$T_m \approx 1/f_{coh} \quad (9.16)$$

9.2 Frequency-Nonselective, Slowly Fading Channel

$$T_s \ll t_{coh} \tag{9.27}$$

or equivalently,

$$B_{\mathcal{D}} \ll R_s \tag{9.28}$$

This means that the channel is **slowly fading**, which imply that it can be treated as a time-invariant channel within the coherence time.

In this subsection a frequency-nonselective channel is investigated. To obtain this situation it is required that the bandwidth of the transmitted signal, denoted W, is much smaller than the coherence bandwidth f_{coh} of the channel,

$$W \ll f_{coh} \tag{9.29}$$

or equivalently,

$$T_m \ll 1/W \tag{9.30}$$

$$\boxed{\boxed{\tilde{z}(t) = \frac{1}{2}\int_{-\infty}^{\infty} \tilde{S}(f)\tilde{H}(f,t)e^{j2\pi ft}df}} \tag{9.26}$$

$$\boxed{z_I(t) + jz_Q(t) = \frac{1}{2}\int_{-\infty}^{\infty}[S_I(f) + jS_Q(f)]\ [H_I(f,t) + jH_Q(f,t)]e^{j2\pi ft}df} \tag{9.33}$$

$$z_I(t) + jz_Q(t) = \frac{1}{2}\int_{-\infty}^{\infty}[S_I(f) + jS_Q(f)] \cdot (H_I + jH_Q)e^{j2\pi ft}df \tag{9.36}$$

$$\begin{aligned} z_I(t) + jz_Q(t) &= \frac{1}{2}\ (s_I(t) + js_Q(t))(H_I + jH_Q) = \\ &= e_s(t)e^{j\theta_s(t)} \cdot ae^{j\phi} = e_z(t)e^{j\theta_z(t)} \end{aligned} \tag{9.37}$$

$$\begin{aligned} z_I(t) + jz_Q(t) &= \frac{1}{2}\,(s_I(t) + js_Q(t))(H_I + jH_Q) = \\ &= e_s(t)e^{j\theta_s(t)} \cdot ae^{j\phi} = e_z(t)e^{j\theta_z(t)} \end{aligned} \tag{9.37}$$

$$\boxed{\boxed{z(t) = ae_s(t)\cos(\omega_c t + \theta_s(t) + \phi)}} \tag{9.38}$$

$$p_a(x) = \frac{2x}{b}\,e^{-x^2/b}, \quad x \geq 0 \quad \text{(Rayleigh distribution)} \tag{9.39}$$

where,

$$E\{a\} = \frac{1}{2}\,\sqrt{\pi b} \tag{9.40}$$

$$E\{a^2\} = b \tag{9.41}$$

and,

$$p_\phi(y) = \begin{cases} 1/2\pi & , \quad -\pi \leq y \leq \pi \\ 0 & , \quad \text{otherwise} \end{cases} \tag{9.42}$$

If we assume uncoded equally likely binary signals over a Rayleigh fading channel ($z_1(t) = as_1(t), z_0(t) = as_0(t)$), then the bit error probability of the ideal coherent ML receiver is ($0 < d^2 = \frac{D^2_{s_1,s_0}}{2E_{b,sent}} \leq 2$)

$$\boxed{\boxed{\boldsymbol{P_b = \int_0^\infty \mathbf{Pr}\{\mathbf{error}|a\}p_a(x)dx = E\{\mathbf{Pr}\{\mathbf{error}|a\}\}}}} \tag{9.43}$$

$$\begin{aligned}
P_b &= \int_0^\infty Q(\sqrt{d^2x^2E_{b,sent}/N_0})\ \frac{2x}{b}\ e^{-x^2/b}dx = \\
&= -e^{-x^2/b}\ Q(x\sqrt{d^2E_{b,sent}/N_0})\Big]_0^\infty - \int_0^\infty (-e^{-x^2/b}) \\
&\quad \left(\frac{-\sqrt{d^2E_{b,sent}/N_0}}{\sqrt{2\pi}}\ e^{-\frac{x^2d^2E_{b,sent}/N_0}{2}}\right) dx = \\
&= \frac{1}{2} - \sqrt{d^2E_{b,sent}/N_0} \cdot \beta \underbrace{\int_0^\infty \frac{e^{-x^2/2\beta^2}}{\beta\sqrt{2\pi}}dx}_{1/2}
\end{aligned} \tag{9.44}$$

$$\mathcal{E}_b = E\{a^2\}E_{b,sent} = bE_{b,sent} \tag{9.45}$$

$$P_b = \frac{1}{2}\left(1 - \sqrt{\frac{d^2\mathcal{E}_b/N_0}{2 + d^2\mathcal{E}_b/N_0}}\right) = \frac{1}{2 + d^2\mathcal{E}_b/N_0 + \sqrt{2 + d^2\mathcal{E}_b/N_0}\sqrt{d^2\mathcal{E}_b/N_0}}$$

$$\underset{\approx}{\overset{\mathcal{E}_b/N_0 \text{ "large"}}{\downarrow}} \quad \frac{1}{2d^2\mathcal{E}_b/N_0} \tag{9.46}$$

where $d^2 = 2$ for antipodal signals and $d^2 = 1$ for orthogonal signals.
Observe the dramatic increase in P_b due to the Rayleigh fading channel. P_b is no longer exponentially decaying in $\mathcal{E}_b/N_0$, it now decays essentially as $(\mathcal{E}_b/N_0)^{-1}$!

EXAMPLE 9.1

Assume that equally likely, binary orthogonal FSK signals, with equal energy, are sent from the transmitter. Hence, $s_i(t) = \sqrt{2E_{b,sent}/T_b}\cos(2\pi f_i t)$ *in* $0 \leq t \leq T_b$, $i = 0, 1$.

These signals are communicated over a Rayleigh fading channel, i.e. the received signal is (see (9.38)),

$$r(t) = a\sqrt{2E_{b,sent}/T_b}\cos(2\pi f_i t + \phi) + N(t)$$

Assume that the incoherent receiver in Figure 5.28 on page 397 is used. From (5.109) it is known that for a given value of a,

$$P_b = \frac{1}{2}\ e^{-a^2 E_{b,sent}/2N_0}$$

since $a^2 E_{b,sent}$ *then is the average received energy per bit.*

For the Rayleigh fading channel, and the same receiver, P_b *can be calculated by using (9.43),*

$$\boxed{\boxed{P_b = \int_0^{\infty} \Pr\{error|a = x\} p_a(x) = E\{\Pr\{error|a\}\}}}$$

$$E\{\Pr\{error|a\}\} = E\left\{\frac{1}{2}\; e^{-a^2 E_{b,sent}/2N_0}\right\} =$$

$$E\left\{\frac{1}{2}\; e^{-a_1^2 E_{b,sent}/2N_0}\right\} \cdot E\left\{e^{-a_2^2 E_{b,sent}/2N_0}\right\}$$

$$P_b = \frac{1/2}{1 + \frac{E_{b,sent}}{N_0} \cdot \frac{E\{a^2\}}{2}} = \frac{1}{2 + \mathcal{E}_b/N_0}$$

Observe the dramatic increase in P_b due to the Rayleigh fading channel. P_b is no longer exponentially decaying in $\mathcal{E}_b/N_0$, it now decays essentially as $(\mathcal{E}_b/N_0)^{-1}$! *As an example, assuming $\mathcal{E}_b/N_0 = 1000$ (30 dB), we obtain*

$$P_b = \begin{cases} 0.5e^{-500} \approx 3.6 \cdot 10^{-218} & , \quad AWGN \\ (1002)^{-1} \approx 10^{-3} & , \quad Rayleigh{+}AWGN \end{cases}$$

DIVERSITY IS NEEDED!